Syntheses, Structural Characterization, and First Electroluminescent Properties of Mono-cyclometalated Platinum(II) Complexes with Greater than Classical $\pi-\pi$ Stacking and Pt−Pt Distances†

Alex S. Ionkin,* William J. Marshall, and Ying Wang

DuPont Central Research & Development, DuPont Displays, Experimental Station, Wilmington, Delaware 19880-0328

Received October 12, 2004

A series of mono-cyclometalated Pt(II) complexes (**9**, **10**, **13**, **15**, and **17**) bearing 2-(3,5-bis(trifluoromethyl)phenyl)-4-methylpyridine (**1**) as the same chromophoric N∧C cyclometalated ligand and the second nonchromophoric bidenate ligands with increasing bulkiness were synthesized by the following steps. The palladium-catalyzed cross-coupling reaction between 2-chloro-4-methylpyridine (**2**) and 3,5-bis(trifluoromethyl)phenylboronic acid (**3**) was used to prepare 2-(3,5-bis(trifluoromethyl)phenyl)-4-methylpyridine (**1**). Di-*tert*-butyl(trimethylsilyl)anylmethylphosphine, *tert*-Bu_2P-CH_2-$SiMe_3$ (**5**), was used as a ligand for the Suzuki coupling. The cyclometalation of **1** by K_2PtCl_4 (**7**) was carried out in $(MeO)_3P{=}O$ (**8**) with the formation of a chloro-bridged dimer N∧CPt(μ-Cl)$_2$PtC∧N (**9**). The reactions of **9** with 2,2,6,6-tetramethylheptane-3,5-dionate (**11**), 1,1,1,3,3,3-hexafluoro-2-pyrazol-1-ylmethylpropan-2-ol (**12**), 2-[(diphenylphosphanyl)methyl]-1,1,1,3,3,3-hexafluoropropan-2-ol (**14**), and 2-[(di-*tert*-butylphosphanyl)methyl]-1,1,1,3,3,3-hexafluoropropan-2-ol (**16**) afforded square-planar Pt(II) complexes **10**, **13**, **15**, and **17**, correspondingly. According to X-ray analyses, the plane-to-plane distances of the $\pi-\pi$ stacked complexes (**10**, **13**, **15**, and **17**) increase from 3.478 Å for **10** to 4.203 Å for **15**. The value of 4.203 Å for aromatic−aromatic $\pi-\pi$ interaction is greater than the usual range of 3.3−3.8 Å for these phenomena. Pt−Pt distances increase from 5.076 Å for **13** to 8.123 Å for **17**. The geometry of complex **17** deviates greatly from square planar and is best described as "bowl-shaped". The effect of an increased $\pi-\pi$ stacking distance on the electroluminescent properties of these Pt compounds is studied. The typical yellow luminescence band associated with the excimers of Pt compounds is absent for complex **15**; however, it shows a green 540 nm electroluminesce band instead. An efficient LED constructed using compound **15** shows green electroluminescence with a peak efficiency of 6 cd/A.

Introduction

Aromatic−aromatic or $\pi-\pi$ interactions are important noncovalent intermolecular forces.[1−3] They play an important role in the binding and conformations from DNA−metal complexes[4,5] to the area of electroluminescence in OLED technology.[6−12] Calculations give an energy of about 2 kJ mol^{-1} for a typical aromatic−aromatic $\pi-\pi$ interaction.[13] There are three different patterns of the stacked arrangements in monoaromatic systems: a perfect face-to-face alignment of atoms; offset or slipped packing; and T-shaped conformation, which is C-H−π interaction (Figure 1).

The face-to-face $\pi-\pi$ interaction, where most of the ring−plane area overlaps, is a rare phenomenon. The usual $\pi-\pi$ interaction is an offset or slipped stacking. The ring normal and the vector between the ring centroids form an angle of around 20° up to centroid−centroid distances of 3.8 Å.[1] The T-shaped mode of $\pi-\pi$ interaction is known for benzene. The stacked structures become increasingly favorable with increasing arene size.[14] Larger systems such as pyrene or coronene show

† DuPont contribution #8551.

* To whom correspondence should be addressed. E-mail: alex.s.ionkin@usa.dupont.com.

(1) Janiak, C. *J. Chem. Soc., Dalton Trans.* **2000**, *21*, 3885.
(2) Roesky, H. W.; Andruh, M. *Coord. Chem. Rev*. **2003**, *236*, 91.
(3) Jones, G. B. *Tetrahedron* **2001**, *57*, 7999.
(4) Yang, F.; Fanwick, P. E.; Kubiak, C. P. *Inorg. Chem*. **2002**, *41*, 4805.
(5) Hunter, C. A.; Singh, J.; Thornton, J. M. *J. Mol. Biol*. **1991**, *218*, 837.
(6) Brooks, J.; Babayan, Y.; Djurovich, P. I.; Adamovich, V.; Tsyba, I.; Bau, R.; Forrest, S.; D'Andrade, B.; Thompson, M. E. Abstracts of Papers, 224th ACS National Meeting, Boston, MA, 2002; American Chemical Society: Washington, DC, 2002.
(7) Sakai, K.; Kurashima, M.; Akiyama, N.; Satoh, N.; Kajiwara, T.; Ito, T. *Acta Crystallogr*. **2003**, *C59*, m349.
(8) Lai, S.-W.; Chan, M. C. W.; Cheung, K.-K.; Che, C.-M. *Inorg. Chem*. **1999**, *38*, 4262.
(9) Lai, S.-W.; Cheung, T.-C.; Chan, M. C. W.; Cheung, K.-K.; Peng, S.-M.; Che, C.-M. *Inorg. Chem*. **2000**, *39*, 255.
(10) Lai, S.-W.; Chan, M. C. W.; Cheung, K.-K.; Peng, S.-M.; Che, C.-M. *Organometallics* **1999**, *18*, 3991.
(11) Lai, S.-W.; Chan, M. C. W.; Cheung, K.-K.; Peng, S.-M.; Che, C.-M. *Organometallics* **1999**, *18*, 3327.
(12) Liu, Z.-H.; He, C.; Duan, C.-Y.; You, X.-Z. *Inorg. Chem. Commun*. **1999**, *2*, 279.
(13) Jorgensen, W. L.; Severance, D. L. *J. Am. Chem. Soc.* **1990**, *112*, 4768.

10.1021/om049211t CCC: $30.25
Publication on Web 01/14/2005

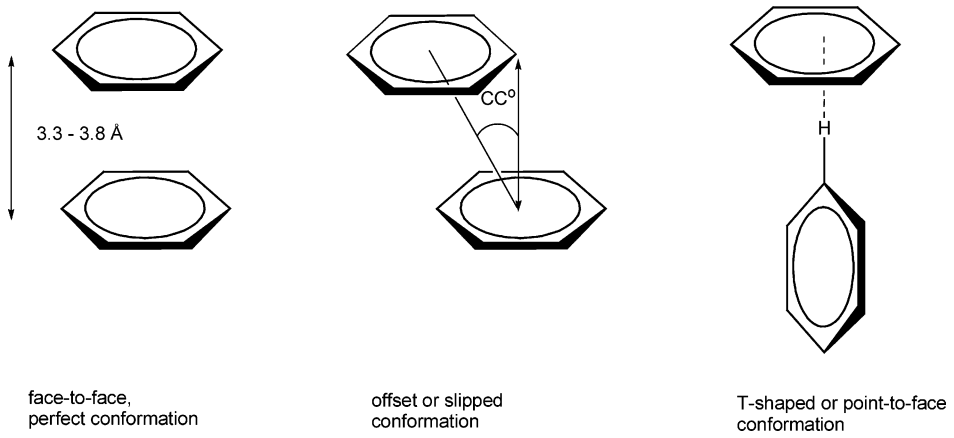

Figure 1. Three general conformations in $\pi-\pi$ interactions of monoaromatic systems.

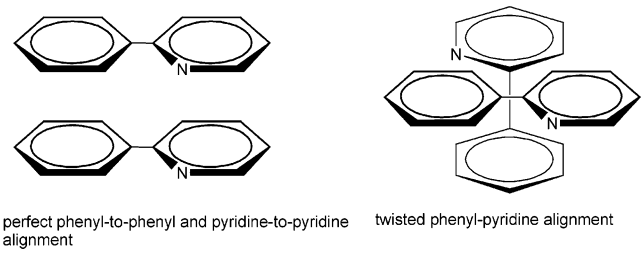

Figure 2. Perfect and twisted alignments of 2-phenylpyridines in $\pi-\pi$ stacking.

the slipped $\pi-\pi$ stacking with the hydrogen atoms roughly over the ring centers.[13,15–17] The introduction of nitrogen into aromatic systems increases the tendency to stack. The 2-phenylpyridine ligands are important features of the cyclometalated complexes of platinum and iridium for luminescent studies,[18,19] where the phenomenon of $\pi-\pi$ stacking correlates with a yellow band in the photo- or electroemission.[20] Bicyclic systems, such as 2-phenylpyridine, have several additional alignments in $\pi-\pi$ stacking (Figures 2 and 3). The perfect phenyl-to-phenyl and pyridine-to-pyridine alignments are again rare. The alignments with twisted orientations of two phenyl−pyridine rings (second picture in Figure 2) are most common.

Two additional alignments resulted upon the rotation of the perfect alignment of 2-phenylpyridine systems (shown in Figure 2) by 180° around the pyridine-to-pyridine $\pi-\pi$ stacking and around phenyl-to-phenyl $\pi-\pi$ stacking (Figure 3).

This report describes the successful breaking of $\pi-\pi$ stacking of mono-cyclometalated Pt(II) compounds with more than a 3.8 Å plane-to-plane distance, resulting in the elimination of the yellow band in the emission of OLED devices. Because of the relatively low energy for a typical $\pi-\pi$ stacking interaction (2 kJ mol^{-1}), the steric bulk of the second auxiliary ligand of square-planar Pt(II) complexes bearing the same cyclometalated phenyl-pyridine ligand was gradually increased to break the $\pi-\pi$ stacking above 3.8 Å, and the changes in emission spectra were recorded. The results are discussed in the following sections.

Results and Discussion

1.1. Synthesis of Mono-cyclometalated Pt(II) Complexes and Structural Studies. 2-(3,5-Bis(trifluoromethyl)phenyl)-4-methylpyridine (**1**) was selected as a ligand for cycloplatination for two reasons: it gives blue emissive bis-cyclometalated Ir(III) complexes, and it gives one of the most intense blue emissive bis-cyclometalated Ir(III) complexes.[21] The palladium-catalyzed Suzuki cross-coupling reaction between 2-chloro-4-methylpyridine (**2**) and 3,5-bis(trifluoromethyl)-phenylboronic acid (**3**) was used to prepare 2-(3,5-bis-(trifluoromethyl)phenyl)-4-methylpyridine (**1**) (Scheme 1).

The synthetic protocol involves Pd_2dba_3 (**4**)/di-*tert*-butyl(trimethylsilyl)anylmethylphosphine (**5**) as the catalyst in the presence of cesium fluoride (**6**) in 1,4-dioxane as solvent.[22]

The cyclometalation of 2-(3,5-bis(trifluoromethyl)-phenyl)-4-methylpyridine (**1**) with potassium tetrachloroplatinate (**7**) was carried out in trimethyl phosphate (**8**). The electrophilic reactions, like cyclometalation, in trimethyl phosphate take place at lower temperatures in many difficult cases.[23] The Pt(II)-bridged dichloride dimer **9** precipitated from the trimethyl phosphate solution, simplifying the purification step (Scheme 2).

Platinum(II) [4,6-bis(trifluoromethyl)-2-(4-methyl-2-pyridinyl-κN)phenyl-κC](2,2,6,6-tetramethyl-3,5-heptanedionato-$\kappa O,\kappa O'$) (**10**) was prepared by the reaction of complex **9** and lithium 2,2,6,6-tetramethylheptane-3,5-dionate (**11**) (Scheme 3).

A crystal of complex **10** suitable for X-ray analysis was grown from pentane. The ORTEP drawing of **10** is shown in Figure 4.

Complex **10** represents the classical case of the twisted $\pi-\pi$ stacking of cyclometalated platinum com-

(14) Goddard, R.; Haenel, M. W.; Herndon, W. C.; Kruger, C.; Zandler, M. *J. Am. Chem. Soc.* **1995**, *117*, 30.
(15) Robertson, J. M.; White, J. G. *J. Chem. Soc.* **1947**, 358.
(16) Kitaigorodski, A. I. *Molecular Crystals and Molecules*; Academic Press: New York, 1973.
(17) Desiraju, G. R.; Gavezzotti, A. *J. Chem. Soc., Chem. Commun.* **1989**, 621.
(18) Lamansky, S.; Djurovich, P.; Murphy, D.; Abdel-Razzaq, F.; Lee, H.-E.; Adachi, C.; Burrows, P. E.; Forrest, S. R.; Thompson, M. E. *J. Am. Chem. Soc.* **2001**, *123*, 4304.
(19) Tamayo, A. B.; Alleyne, B. D.; Djurovich, P. I.; Lamansky, S.; Tsyba, I.; Ho, N. N.; Bau, R.; Thompson, M. E. *J. Am. Chem. Soc.* **2003**, *125*, 7377.
(20) Brooks, J.; Babayan, Y.; Lamansky, S.; Djurovich, P. I.; Tsyba, I.; Bau, R.; Thompson, M. E. *Inorg. Chem.* **2002**, *41*, 3055.
(21) Grushin, V.; Petrov, V. A. PCT Int. Appl. 2003, WO 2003069961.
(22) Ionkin, A. S.; Marshall, W. J. *J. Organomet. Chem.* **2004**, *689*, 1057.
(23) Cowley, A. H.; Norman, N. C.; Pakulski, M. *Inorg. Synth.* **1990**, *27*, 235.

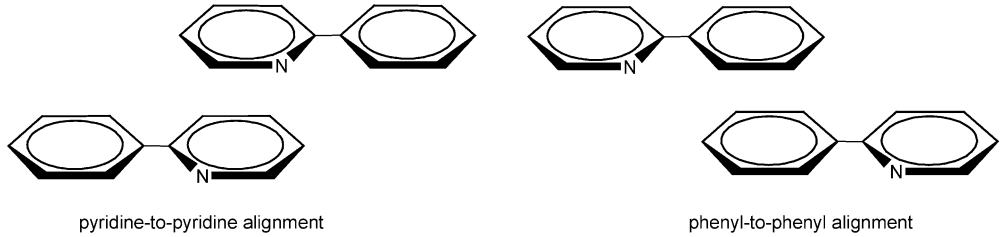

Figure 3. Pyridine-to-pyridine and phenyl-to-phenyl alignments of 2-phenylpyridines in $\pi-\pi$ stacking.

Scheme 1

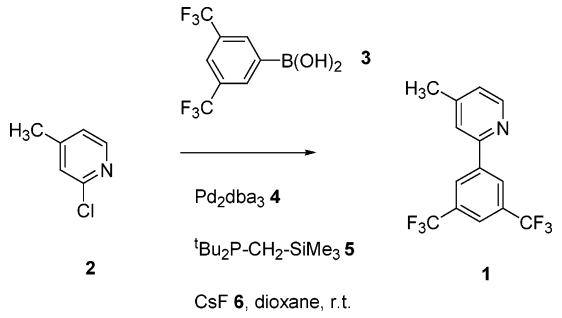

Scheme 2

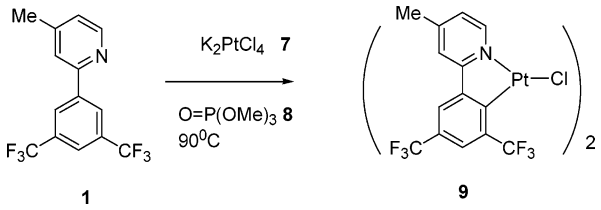

Scheme 3

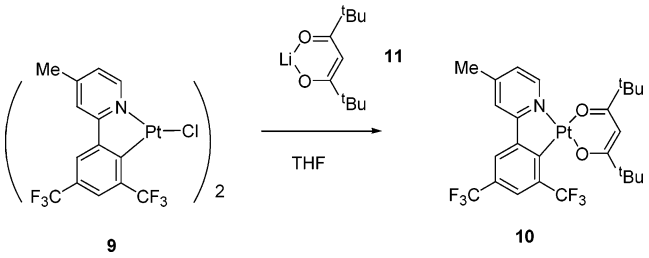

pounds. The plane-to-plane distance is 3.478 Å. The two phenyl-pyridine rings are twisted by 46.6° relative to each other (Figure 5). The centroid−centroid distance between the two pyridine fragments is 4.410 Å. The ring normal and the vector between pyridine ring centroids form an angle of 37.9°. The centroid−centroid distance between two phenyl fragments is 3.820 Å. The ring normal and the vector between phenyl ring centroids form an angle of 20.6°. The Pt−Pt distance is 5.084 Å (Table 1). There is very little distortion from the square-planar geometry of **10** (second row of Table 2). The phenyl and pyridine moiety of the phenyl-pyridine ligand of **10** is only slightly bowed relative to each other with an angle of 5.3° (first row of Table 2).

To increase the steric bulk on the side of the auxiliary ligand, 1,1,1,3,3,3-hexafluoro-2-pyrazol-1-ylmethylpropan-2-ol (**12**) was used instead of lithium 2,2,6,6-tetramethylheptane-3,5-dionate (**11**) in the ligand exchange reaction of starting complex **9** (Scheme 4). In contrast to acetylacetonate complexes, like **10**, 1,1,1,3,3,3-hexafluoro-2-pyrazol-1-ylmethylpropan-2-ol (**12**) forms a nonplanar six-membered ring with the metal. The

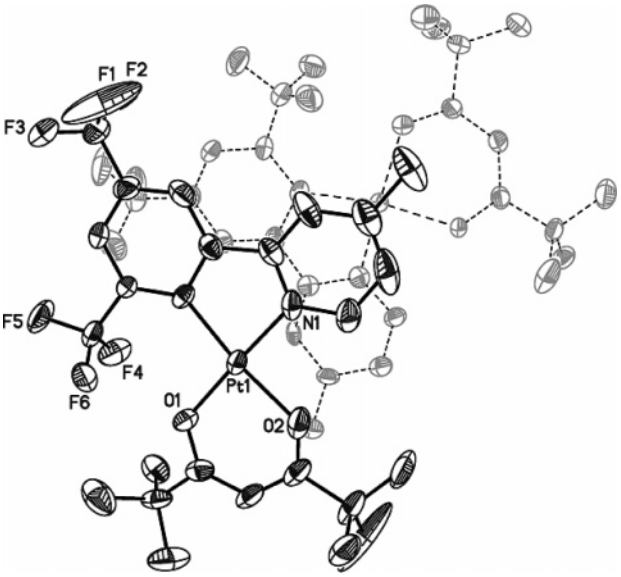

Figure 4. ORTEP drawing of the $\pi-\pi$ stacked platinum complex **10**. This is an example of the classical twisted phenyl-pyridine alignment in $\pi-\pi$ stacking. The plane-to-plane distance is 3.478 Å. The Pt−Pt distance is 5.084 Å.

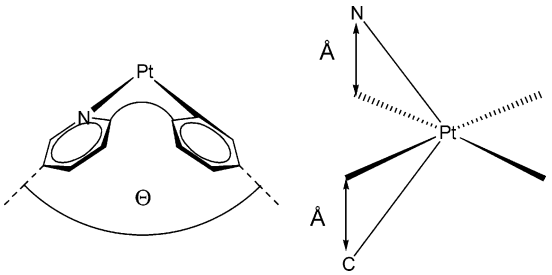

Figure 5. Outstanding features of the cyclometalated ring system in complexes **10**, **13**, **15**, and **17**: the bow formed by phenyl and pyridine moieties of the phenyl-pyridine ligand (left picture) and the deviation of platinum from square-planar geometry (right picture).

Scheme 4

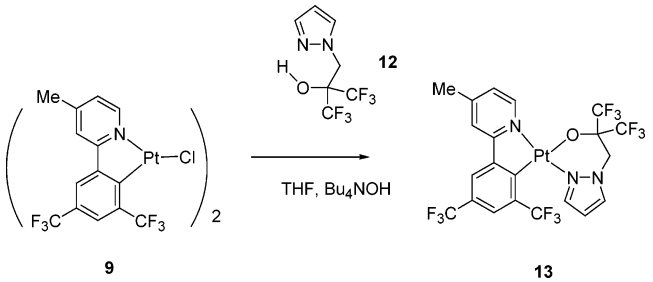

pyrazol moiety and two CF_3 groups have a tendency to orient themselves outside the plane of the six-membered ring and push the second molecule participating in $\pi-\pi$ stacking farther away.

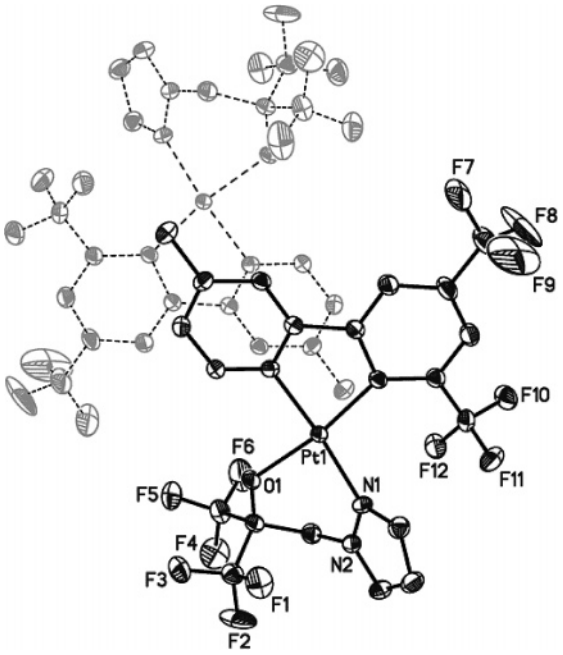

Figure 6. ORTEP drawing of the $\pi-\pi$ stacked platinum complex **13**. This is the case of pyridine-to-pyridine alignment in $\pi-\pi$ stacking. The plane-to-plane distance is 3.504 Å. The Pt−Pt distance is 5.076 Å.

The single crystal of complex **13** suitable for X-ray analysis was grown from pentane. The ORTEP drawing of **13** is shown in Figure 6.

Platinum(II) [4,6-bis(trifluoromethyl)-2-(4-methyl-2-pyridinyl-κN)phenyl-κC],[α,α-bis(trifluoromethyl)-2-pyrazol-1-ylmethylpropan-2-olato-$\kappa N1$,κO] (**13**) was isolated as the trans-N,N-isomer. There is pyridine-to-pyridine orientation in $\pi-\pi$ stacking of cyclometalated platinum complex **13**. The plane-to-plane distance is 3.504 Å, which is slightly higher than for complex **10**. The centroid−centroid distance between the two pyridine fragments is 3.581 Å. The ring normal and the vector between pyridine ring centroids form an angle of 11.9°. The phenyl fragments are located too far apart (more than 10 Å) to participate in a $\pi-\pi$ interaction. The Pt−Pt distance has been found to be close to the value found for compound **10**: 5.076 Å (Table 1). However, the distortion from square-planar geometry has increased for **13**. The nitrogen atom (N8) deviated by 0.383 Å from the mean plane of the trans atoms (O−Pt−N and C−Pt−N) (second row of Table 2). The phenyl and pyridine moieties of the phenyl-pyridine ligand of **13** are bowed relative to each other with an angle of 10.3°.

To separate the $\pi-\pi$ stacking of the aromatic rings even further, 2-[(diphenylphosphanyl)methyl]- 1,1,1,3,3,3-hexafluoropropan-2-ol (**14**) was used instead of 1,1,1,3,3,3-hexafluoro-2-pyrazol-1-ylmethylpropan-2-ol (**12**) in the reaction with platinum precursor **9** (Scheme 5). The rationale behind this experiment was that two phenyl groups at the phosphorus atom in addition to two trifluoromethyl groups will push the $\pi-\pi$ stacking planes beyond energetically favorable interaction.

According to the results of the X-ray analysis (Figure 7), complex **15** is the trans-N,P-isomer. This is the closest to the mode of phenyl-to-phenyl alignment of $\pi-\pi$ stacking, but the distance is long. The plane-to-plane distance in compound **15** was found to be 4.203 Å. This value is out of the range of 3.3−3.8 Å accepted for the phenomenon of $\pi-\pi$ stacking.[1] The Pt−Pt distance was found to be 7.028 Å. The centroid−centroid distance between the two phenyl fragments is 4.237 Å, which is also above the normal range found in $\pi-\pi$ stacking.[1] The ring normal and the vector between the pyridine ring centroids form an angle of 7.3°. The pyridine fragments are located too far apart (more than 10 Å) to participate in a $\pi-\pi$ interaction. The distortion from square-planar geometry is moderate for **15**. The nitrogen atom (N1) deviates by 0.191 Å from the mean plane of the trans atoms (O−Pt−P and C−Pt−N) (second row of Table 2). The phenyl and pyridine moiety

Table 1. $\pi-\pi$ Stacking Parameters for Compounds 10, 13, 15, and 17

	10	13	15	17
plane-to-plane distance, Å	3.478	3.504	4.203	3.533
Pt−Pt distances, Å	5.084	5.076	7.028	8.123
orientation of two molecules relative to each other in the crystal cell	twisted phenyl-pyridine alignment (46.6°)	pyridine-to-pyridine alignment (180°)	phenyl-to-phenyl alignment (180°)	pyridine-to-pyridine alignment (180°)
centroid−centroid contacts between two pyridine fragments, Å	4.410	3.581	>10 Å	3.784
centroid−centroid contacts between two phenyl fragments, Å	3.820	>10 Å	4.237	>10 Å
pyridine/pyridine displacement: angle between the ring−centroid vector and the ring normal to one of the pyridine planes	37.9	11.9	>10 Å to measure	21.0
phenyl/phenyl displacement: angle between the ring−centroid vector and the ring normal to one of the phenyl planes	20.6	>10 Å to measure	7.3	>10 Å to measure

Table 2. Distortion of the Ring System in 10, 13, 15, and 17

	10	13	15	17
θ (deg), dihedral angle between the mean planes of the six-membered rings of the phenyl-pyridine ligand	5.3	10.7	7.1	19.7
deviations (Å) from the mean plane of the trans atoms (O−Pt−O, O−Pt−N, or O−Pt−P)	N1 = −0.068, C12 = 0.112, N27 = −0.167, C38 = 0.085	N8 = −0.383, C19 = 0.017	N1 = −0.191, C12 = −0.048	N1= 0.866, C12 = −0.006

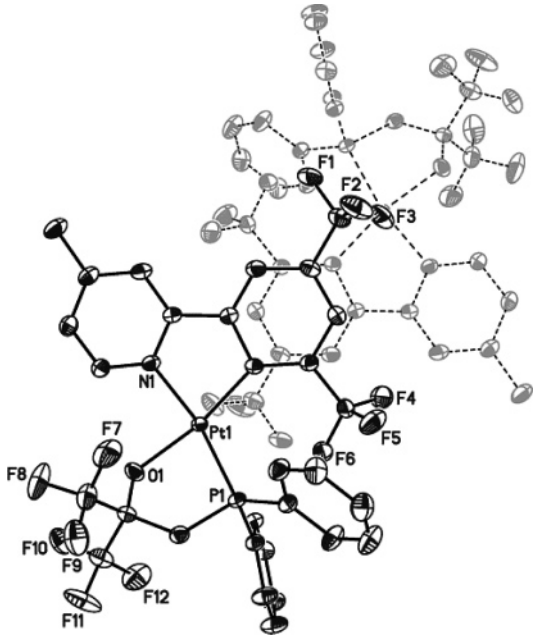

Figure 7. ORTEP drawing of the $\pi-\pi$ stacked platinum complex **15**. This is the closest to the mode of phenyl-to-phenyl alignment of $\pi-\pi$ stacking but far way. The plane-to-plane distance is 4.203 Å. The Pt−Pt distance is 7.028 Å.

Scheme 5

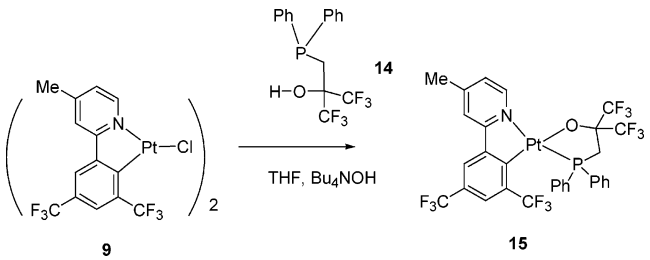

Scheme 6

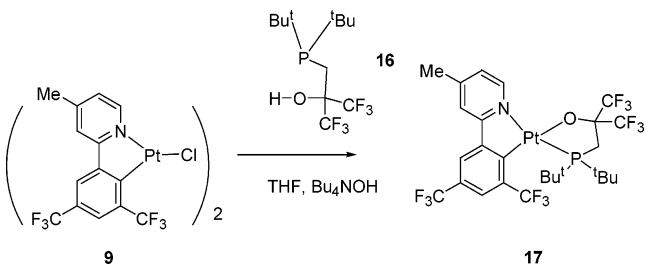

of the phenyl-pyridine ligand of **15** are bowed relative to one another with an angle of 7.1°.

To spread the Pt-nuclei farther apart in the lattice, the phenyl groups at the phosphorus in **15** were replaced by *tert*-butyl groups as in complex **17** (Scheme 6). The reaction between platinum precursor **9**, 2-[(di-*tert*-butylphosphanyl)methyl]-1,1,1,3,3,3-hexafluoropropan-2-ol (**16**), and tetrabutylammonium hydroxide in a solution of THF afforded the desired complex **17**.

According to the results of the X-ray analysis (Figures 8 and 9), complex **17** is the trans-N,P-isomer. The Pt−Pt distance in complex **17** is the longest in this study at 8.123 Å. There is the pyridine-to-pyridine alignment of $\pi-\pi$ stacking in complex **17**. The plane-to-plane distance is 3.533 Å. However, the main feature of compound **17** is the distortion of the square-planar

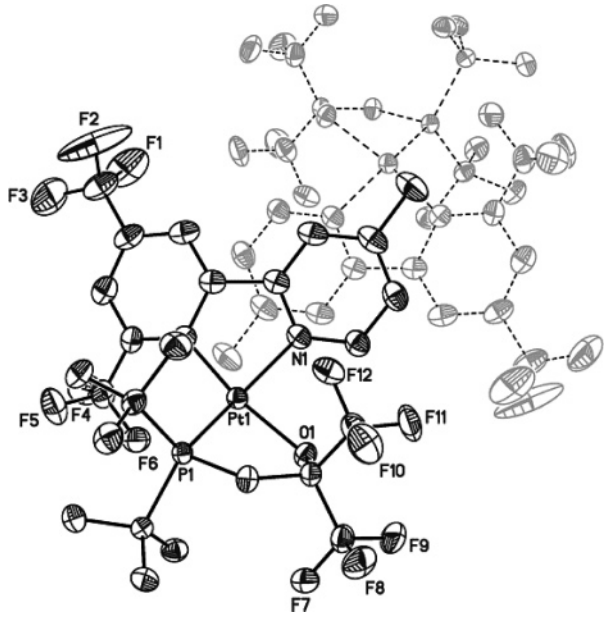

Figure 8. ORTEP drawing of the $\pi-\pi$ stacked platinum complex **17**. This is the case of pyridine-to-pyridine alignment in $\pi-\pi$ stacking. The plane-to-plane distance is 3.533 Å. The Pt−Pt distance is 8.123 Å.

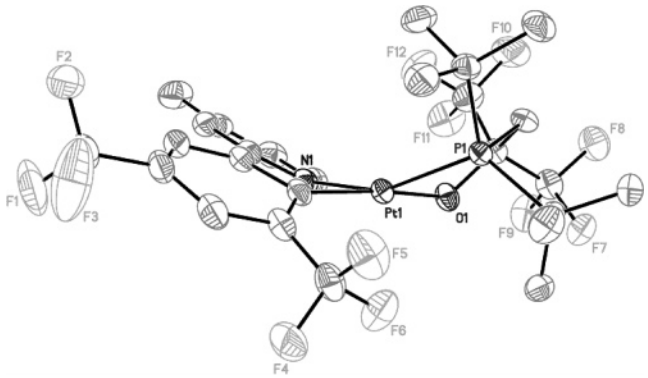

Figure 9. ORTEP drawing of the platinum complex **17** showing "bowl-shaped" conformation. Complex **17** is greatly distorted. The angle between the mean planes of the six-membered rings of the phenyl-pyridine ligand of **17** is 19.7°.

geometry around the platinum atom and a deviation of the phenyl-pyridine ligand from planarity. The angle between the mean planes of the six-membered rings of the phenyl-pyridine ligand of **17** is 19.7°. The geometry of **17** deviates greatly from square planar (Figures 9 and 5). The nitrogen atom (N1) again deviates by 0.866 Å from the mean plane of the trans atoms (O−Pt−P and C−Pt−N) (second row of Table 2). It would be best to describe the geometry as "bowl-shaped" not square planar.[24]

A Cambridge Structural Database (CSD) search has been performed using QUEST3D routine to evaluate Pt−Pt distances of the mono-cyclometalated $\pi-\pi$ stacked Pt complexes containing a parent 2-phenylpyridine moiety. The results of the search are as follows: the smallest Pt−Pt distance was 3.528 Å[25] and the longest Pt−Pt distance was 8.679 Å.[26] The average Pt−Pt

(24) Corey, S.; Jun, P.; Suning, W. *Eur. J. Inorg. Chem.* **2002**, 1390.
(25) Chassot, L.; Muller, E.; Zelewsky, von A. *Inorg. Chem.* **1984**, *23*, 4249.
(26) DePriest, J.; Zheng, G. Y.; Goswami, N.; Eichhorn, D. M.; Woods, C.; Rillema, D. P. *Inorg. Chem.* **2000**, *39*, 1955.

distance was 6.72 Å among the eight found structures.[27−31] Thus, complexes **15** and **17** from this investigation possess above average Pt−Pt distances. It appears that Pt−Pt measurement is the simplest test of the bulkiness of the Pt complex. However, it could not be used alone without analyzing the distortion of a molecule or $\pi-\pi$ stacking; for example, complex **17** in our study has the longest Pt−Pt distance of 8.123 Å, but because of substantial distortion (Table 2) of the cyclometalated moiety of the complex and the deviation from planarity of the square Pt geometry, complex **17** is a mediocre photoemitter.

Several patterns of aromatic−aromatic $\pi-\pi$ interactions and different Pt−Pt distances in complexes **10**, **13**, **15**, and **17** were detected by X-ray analysis. Tables 1 and 2 summarize the $\pi-\pi$ stacking parameters and distortion values for compounds **10**, **13**, **15**, and **17**. The initial correlations with OLED performance made from them will be discussed in the next section.

1.2. Electroluminescent and Photoluminescent Properties of Mono-cyclometalated Pt(II) Complexes. Organometallic compounds containing Ir and Pt atoms represent a new class of electroluminescent materials for light-emitting diodes.[18,32−44] Highly efficient devices can be fabricated from these emitters either as neat film[36−38] or in a guest−host system. The luminescent states of these compounds usually contain strong metal-to-ligand charge transfer (MLCT) character. The spin−orbital interaction of the heavy Ir, Pt atom introduces mixed singlet/triplet character in the MLCT emitting state. The triplet character allows the electron−hole recombination statistics to approach the theoretical limit of 100% instead of the 25% limit with the singlet state. The metal-to-ligand charge transfer nature of the emitting state allows the facile tuning of the luminescent wavelength by the substitution of donor and acceptor groups on the organic ligands. Emitters with luminescence wavelength ranging from near blue to deep red have been synthesized.[18,34−44]

Scheme 7

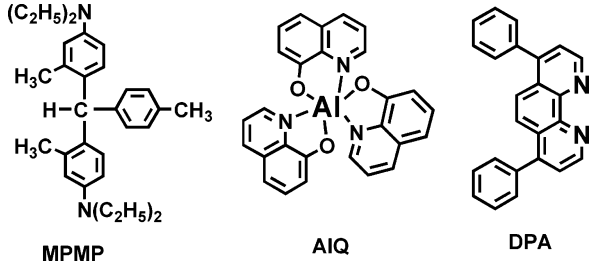

While most of the high-efficiency organometallic emitters are based on Ir compounds, Pt-based emitters have also been reported.[45,46] LEDs built with Pt compounds as the emitter usually show luminescence in the blue region plus additional yellow-orange luminescence in the 580−600 nm region. The blue luminescence is attributed to the monomer emission, and the yellow-orange emission is generally attributed to the excimer emission.[45,46] The facile formation of excimers for the Pt compounds is presumably due to their square-planar geometry, which promotes intermolecular stacking.

Electroluminescent devices were made using compounds **10**, **15**, and **17** as the emitters. The device configuration consists of ITO as the anode, MPMP (300 Å) as the hole transport material, Pt emitters, DPA (100 Å) as the electron transport material, AlQ(300 Å) as the electron injection material, and LiF/Al as the cathode. Molecular structures of the materials used are shown in Scheme 7.

Table 3 summarizes the electroluminescent and photoluminescent properties of these Pt compounds. Compound **15** shows green electroluminescence at 540 nm, while compound **10** gives an additional yellow peak at 580 nm. Compound **17** shows an electroluminescence peak at 560 nm, which may be the convolution of the 540 and 580 nm peak. Compound **15** shows a reasonable efficiency of 6 cd/A without any further device optimization. The onset voltage is relatively high, 19.5 V at 100 cd/m^2, which may be further reduced by optimizing device structure. The voltage dependence of the electroluminescence efficiency and radiance is shown in Figure 10.

Figure 11 shows the absorption, photoluminescence, and electroluminescence spectra of compound **15**. As can be seen, in methylene chloride solution the Pt compound emits blue light with a peak at 405 nm, while the electroluminescence peak is at 540 nm. We note all three Pt compounds show the same 405 nm emission in solution (Table 1), reflecting the fact that they all have the same emissive phenylpyridine ligand. The detailed photophysics of Pt compounds can be extremely complicated and is not pursued in this paper. Our tentative interpretation is that the 405 nm peak may be attributed to the Pt monomer emission, basically from the phenylpyridine ligand with some perturbation by the Pt atom. The 540 nm electroluminescence band

(27) Mdleleni, M. M.; Bridgewater, J. S.; Watts, R. J.; Ford, P. C. *Inorg. Chem.* **1995**, *34*, 2334.
(28) Kvam, P.; Engebretsen, T.; Maartmann-Moe, K.; Songstad, *J. Acta Chem. Scand*. **1996**, *50*, 107.
(29) Balashev, K. P.; Engebretsen, T.; Kvam, P.-I.; Maartmann-Moe, K.; Puzyk, M. V.; Songstad, *J. Acta Chem. Scand*. **1996**, *50*, 1108.
(30) Okada, T.; EI-Mehasseb, I. M.; Kodaka, M.; Tomohiro, T.; Okamoto, K. *J. Med. Chem*. **2001**, *44*, 4661.
(31) Shi, J.-C.; Chao, H.-Y.; Fu, W.-F.; Peng, S.-M.; Che, C.-M. *J. Chem. Soc., Dalton Trans*. **2000**, 3128.
(32) Baldo, M. A.; O'Brien, D. F.; You, Y.; Shoustikov, A.; Sibley, S.; Thompson, M. E.; Forrest, S. R. *Nature* **1998**, *395*, 151.
(33) Baldo, M. A.; Lamansky, S.; Burrows, P. E.; Thompson, M. E.; Forrest, S. R. *Appl. Phys. Lett.* **1999**, *75*, 4.
(34) Holmes, R. J.; Forrest, S. R.; Tung, Y.-J.; Kwong, R. C.; Brown, J. J.; Garon, S.; Thompson, M. E. *Appl. Phys. Lett.* **2003**, *82*, 2422.
(35) Adachi, C.; Baldo, M. A.; Forrest, S. R.; Lamansky, S.; Thompson, M. E.; Kwong, R. C. *Appl. Phys. Lett.* **2001**, *78*, 1622.
(36) Grushin, V. V.; Herron, N.; LeCloux, D. D.; Marshall, W. J.; Petrov, V. A.; Wang, Y. *Chem. Commun*. **2001**, 1494.
(37) Wang, Y.; Herron, N.; Grushin, V. V.; LeCloux, D.; Petrov, V. *Appl. Phys. Lett.* **2001**, *79*, 449.
(38) Grushin, V. V.; LeCloux, D. D.; Petrov, V. A.; Wang, Y. U.S. Patent 6,670,645.
(39) Su, Y.-J.; Huang, H.-L.; Li, C.-L.; Chien, C.-H.; Tao, Y.-T.; Chou, P.-T.; Datta, S.; Liu, R.-S. *Adv. Mater*. **2003**, *15*, 884.
(40) Lo, S.-C.; Male, N. A. H.; Markham, J. P. J.; Magennis, S. W.; Burn, P. L.; Salata, O. V.; Samuel, I. D. W. *Adv. Mater.* **2002**, *14*, 975.
(41) Xie, H. Z.; Liu, M. W.; Wang, O. Y.; Zhang, X. H.; Lee, C. S.; Hung, L. S.; Lee, S. T.; Teng, P. F.; Kwong, H. L.; Zheng, H.; Che, C. M. *Adv. Mater.* **2001**, *13*, 1245.
(42) Duan, J.-P.; Sun, P.-P.; Cheng, C.-H. *Adv. Mater*. **2003**, *15*, 224.
(43) Watanabe, T.; Nakamura, K.; Kawami, S.; Fukuda, Y.; Tsuji, T.; Wakimoto, T.; Miyaguchi, S. In *Organic light-emitting materials and devices IV*; Kafafi, Z. H., Ed.; Proc. of SPIE, 2001; Vol. 4105, p 175.
(44) Ikai, M.; Tokito, S.; Sakamoto, Y.; Suzuki, T.; Taga, Y. *Appl. Phys. Lett*. **2001**, *79*, 156.
(45) Adamovich, V.; Brooks, J.; Tamayo, A.; Alexander, A. M.; Djurovich, P. I.; D'Andrade, B. W.; Adachi, C.; Forrest, S. R.; Thompson, M. E. *New J. Chem.* **2002**, *26*, 1171.
(46) D'Andrade, B. W.; Brooks, J.; Adamovich, V.; Thompson, M. E.; Forrest, S. R. *Adv. Mater*. **2002**, *14*, 1033.

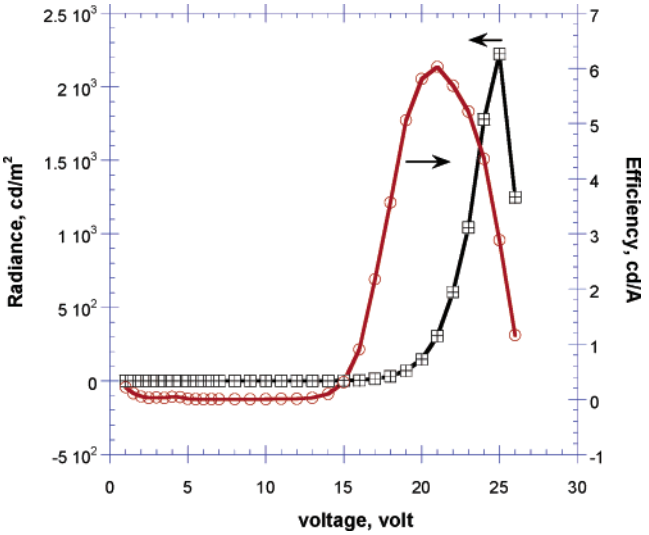

Figure 10. Voltage dependence of the electroluminescence efficiency (cd/A) and radiance (cd/m^2) of compound **15**.

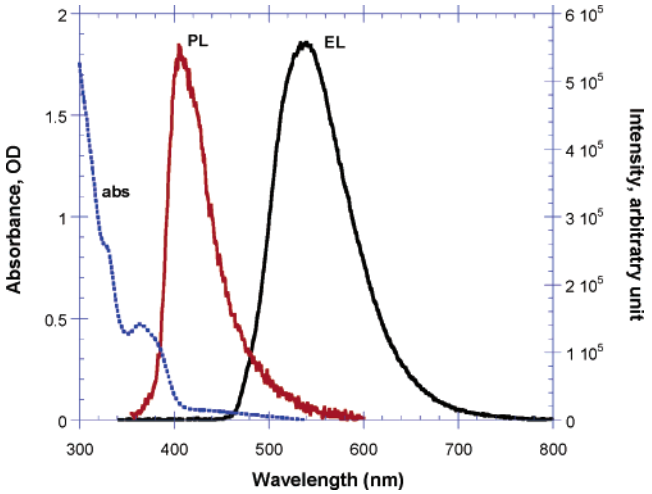

Figure 11. Absorption (dashed line), photoluminescence (PL), and electroluminescence (EL) spectra of compound **15**. The photoluminescence spectrum was taken in methylene chloride solution using 350 nm excitation.

is due to intermolecular interaction of the Pt compounds in the solid state. Its peak position is different from the 580−600 nm excimer emission generally observed for other Pt compounds.[45−48]

For compound **10**, the electroluminescence spectrum either is red-shifted or shows an additional peak in the 580 nm region. The comparison of the electroluminescence spectra of **10** and **15** is shown in Figure 12.

Although films deposited by thermal evaporation are usually amphorous or polycrystalline, the single-crystal structural data can still be useful in terms of providing a guide to the natural tendency of how molecules pack together in the solid state. On the basis of the X-ray data summarized in Tables 1 and 2, we note that compound **15** in general shows a larger intermolecular

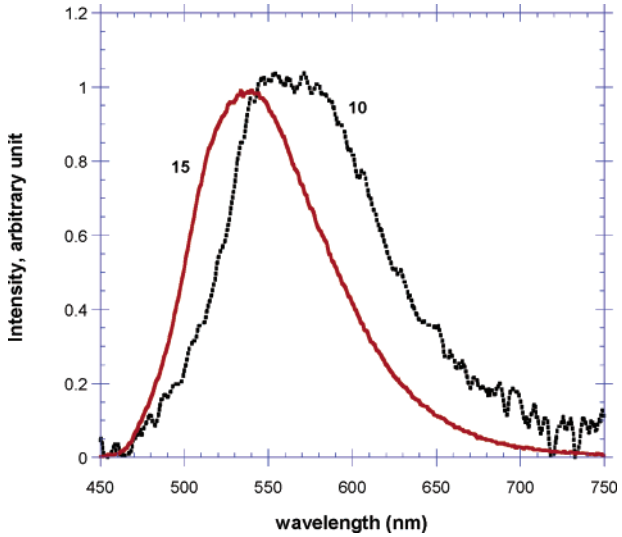

Figure 12. Comparison of the electroluminescence spectra of compounds **15** and **10**.

distance than compound **10**. For example, the plane-to-plane distance is 4.203 Å for **15** compared to 3.478 Å for **10**; the Pt−Pt distance is 7.028 Å for **15** compared to 5.084 Å for **10**. The larger intermolecular distance is presumably due to the bulkier 2-[(diphenylphosphanyl)-methyl]-1,1,1,3,3,3-hexafluoropropan-2-ol (**14**) ligand incorporated in complex **15**. This increased intermolecular distance did not eliminate the aggregation effect of Pt compounds in the solid-state electroluminescence spectrum, as evidenced by the appearance of the 540 nm electroluminescence band, which is different from the monomer band at 405 nm. However, the increased separation does seem to either eliminate the 580−600 nm yellow band or cause it to shift to higher energy. It is known that the excimer emission wavelength is sensitive to the packing geometry of the molecules as well as the intermolecular distance. In general, increased intermolecular separation will destabilize the excimer and cause the emission wavelength to shift to higher energy. Qualitatively, this is consistent with the current observation. Further detailed photophysical studies are needed to gain a complete quantitative understanding of the problem.

Summary

The $\pi-\pi$ stacking of mono-cyclometalated Pt(II) complexes was broken above 3.8 Å plane-to-plane distances by increasing the steric bulk of the second auxiliary ligand in complexes bearing the same cyclometalated phenyl-pyridine ligand. By doing so, this did not eliminate the long-wavelength electroluminescence band in OLED devices, but it did change its emission wavelength to higher energies (540 nm). Our tentative conclusion is that the steric bulkiness did not totally eliminate the intermolecular interaction of the Pt compounds; rather, it weakens the intermolecular in-

Table 3. Electroluminescent Device Data and Photoluminescent Properties of Pt(II) Complexes

Pt(II) complex	EL peak efficiency, cd/A	EL peak radiance, cd/m2	electroluminescence peaks, nm	photoluminescence peaks, nm	PL quantum yields, in methylene chloride
10	1.2	200	540+580	405	0.0089
15	6	2000	540	405	0.017
17	0.15	130	560	405	0.0069

teraction and shifts the aggregate emission to shorter wavelength.

Experimental Section

General Procedures. All the operations related to catalysts were carried out under an argon atmosphere using standard Schlenk techniques. Anhydrous solvents were used in the reactions. Solvents were distilled from drying agents or passed through alumina columns under an argon or nitrogen atmosphere. 3,5-Bis-trifluoromethylphenylboronic acid, 2-chloro-4-methylpyridine, Pd_2dba_3, cesium fluoride, 1,4-dioxane, lithium 2,2,6,6-tetramethylheptane-3,5-dionate, trimethyl phosphate, 55−60% solution of tetrabutylammonium hydroxide in water, and potassium tetrachloroplatinate(II) were purchased from Aldrich.

2-(3,5-Bis(trifluoromethyl)phenyl)-4-methylpyridine (1). 3,5-Bis(trifluoromethyl)phenylboronic acid (**3**) (15.0 g, 0.05815 mol), 7.42 g (0.05816 mol) of 2-chloro-4-methylpyridine (**2**), 17.43 g (0.1148 mol) of cesium fluoride (**6**), 0.53 g (0.000579 mol) of tris(dibenzylideneacetone)dipalladium(0) (**4**), 0.33 g (0.00142 mol) of di-*tert*-butyl(trimethylsilyl)methylphosphine (**5**), and 100 mL of 1,4-dioxane were stirred at room temperature for 12 h. The reaction mixture was filtered, and the solvent was removed under vacuum. The resulting mixture was purified by chromatography on silica gel with the eluent petroleum ether/ethyl ether at 10:0.5. Yield of 2-(3,5-bis-(trifluoromethyl)phenyl)-4-methylpyridine (**1**) was 16.18 g (91%) as a colorless liquid. ^{1}H NMR (500 MHz, C_6D_6): δ 2.56 (s, 3H, Me), 7.11 (s, 1H, arom-H), 7.51 (s, 1H, arom-H), 7.90 (s, 1H, arom-H), 8.45−8.55 (m, 3H, arom-H). ^{19}F NMR (377 MHz, $CDCl_3$): δ −63.35 (s, 3F, CF_3), − 63.36 (s, 3F, CF_3). Anal. Calcd for C14H9F6N: C, 55.09; H, 2.97; N, 4.59. Found: C, 55.01; H, 3.12; N, 4.44.

Platinum(II) Di-μ-chlorobis[4,6-bis(trifluoromethyl)-2-(4-methyl-2-pyridinyl-κN)phenyl-κC] (9). 2-(3,5-Bis(trifluoromethyl)phenyl)-4-methylpyridine (**1**) (12.00 g, 0.0376 mol), 18.27 g (0.0376 mol) of potassium tetrachloroplatinate-(II) (**7**), and 200 mL of trimethyl phosphate (**8**) were stirred at 90 °C for 18 h under a flow of nitrogen. The resultant precipitate was filtered and dried under 1.0 mm vacuum. The yield of the dimer **9** was 15.7 g (78.11%) as a yellow powder. The above crude chloride-bridged dimer was used without further purification in the next steps according to established practice in cyclometalated platinum research.[20]

Platinum(II) [4,6-Bis(trifluoromethyl)-2-(4-methyl-2-pyridinyl-κN)phenyl-κC](2,2,6,6-tetramethyl-3,5-heptanedionato-$\kappa O,\kappa O'$) (10). Platinum(II) di-μ-chlorobis-[4,6-bis(trifluoromethyl)-2-(4-methyl-2-pyridinyl-κN)phenyl-κC] (**9**) (3.72 g, 0.00348 mol), 6.62 g (0.0347) of lithium 2,2,6,6-tetramethylheptane-3,5-dionate (**11**), and 30 mL of THF were refluxed for 2 h under argon atmosphere. The reaction mixture was poured in 200 mL of water and extracted by 200 mL of diethyl ether twice. The extracts were dried over magnesium sulfate overnight. The solvent was removed in a rotavapor and the residue was purified by chromatography on silica gel with the eluent petroleum ether/ethyl ether at 10:0.5. Yield of platinum(II) [4,6-bis(trifluoromethyl)-2-(4-methyl-2-pyridinyl-κN)phenyl-κC],(2,2,6,6-tetramethyl-3,5-heptanedionato-$\kappa O,\kappa O'$) (**10**) was 2.14 g (45.05%) as a yellow solid with no mp until 200 °C. ^{1}H NMR (500 MHz, CD_2Cl_2): δ 1.11 (s, 9H t-Bu), 1.20 (s, 9H t-Bu), 2.40 (s, 3H, Me), 5.90 (s, 1H, H−C=), 7.00−9.10 (m, 5H, arom-H). ^{19}F NMR (377 MHz, CD_2Cl_2): δ −59.41 (s, 6F, CF_3), − 63.31 (s, 6F, CF_3). Anal. Calcd for $C_{25}H_{27}F_6NO_2Pt$ (MW: 682.56): C, 43.99; H, 3.99; N, 2.05. Found: C, 44.13; H, 4.08; N, 2.31.

Platinum(II) [4,6-Bis(trifluoromethyl)-2-(4-methyl-2-pyridinyl-κN)phenyl-κC],[α,α-bis(trifluoromethyl)-2-pyrazol-1-ylmethylpropan-2-olato-$\kappa N1,\kappa O$] (13). Platinum(II) di-μ-chlorobis[4,6-bis(trifluoromethyl)-2-(4-methyl-2-pyridinyl-κN)phenyl-κC] (**9**) (4.0 g, 0.000374 mol), 3.71 g (0.0150 mol) of 1,1,1,3,3,3-hexafluoro-2-pyrazol-1-ylmethylpropan-2-ol (**12**), 7.76 g of a 55−60% solution of tetrabutylammonium hydroxide in water, and 20 mL of THF were refluxed for 2 h under argon atmosphere. The reaction mixture was poured into 200 mL of the water and extracted by 200 mL of diethyl ether twice. The extracts were dried over magnesium sulfate overnight. The solvent was removed in a rotavapor, and the residue was purified by chromatography on silica gel with the eluent petroleum ether/ethyl ether at 10:0.5. Yield of platinum(II) [4,6-bis(trifluoromethyl)-2-(4-methyl-2-pyridinyl-κN)phenyl-κC],[α,α-bis(trifluoromethyl)-2-pyrazol-1-ylmethylpropan-2-olato-$\kappa N1,\kappa O$] (**13**) was 3.10 g (55.56%) as a yellow solid with no mp until 200 °C. ^{1}H NMR (500 MHz, CD_2Cl_2): δ 2.50 (s, 3H, Me), 4.80 (s, 2H, CH2), 6.40−8.90 (m, 8H, arom-H). ^{19}F NMR (377 MHz, CD_2Cl_2): δ −57.19 (s, 3F, CF_3), − 63.35 (s, 3F, CF_3), − 77.21 (s, 6F, CF_3). Anal. Calcd for $C_{21}H_{13}F_{12}N_3OPt$ (MW: 746.41): C, 33.79; H, 1.76; N, 5.63. Found: C, 34.02; H, 2.00; N, 5.62.

Platinum(II) [4,6-Bis(trifluoromethyl)-2-(4-methyl-2-pyridinyl-κN)phenyl-κC], [3-(diphenylphosphino)-1,1,1-trifluoro-2-(trifluoromethyl)-2-propanolato-$\kappa O,\kappa P$] (15). (1.77 g, 0.00166 mol) Platinum(II) di-μ-chlorobis[4,6-bis(trifluoromethyl)-2-(4-methyl-2-pyridinyl-κN)phenyl-κC] (**9**) 1.21 g (1.77 g, 0.00166 mol), 0.0033 mol of 2-[(diphenylphosphanyl)-methyl]-1,1,1,3,3,3-hexafluoropropan-2-ol (**14**), 1.72 g of a 55−60% solution of tetrabutylammonium hydroxide in water, and 20 mL of THF were refluxed for 2 h under argon atmosphere. The reaction mixture was poured into 200 mL of the water and extracted by 200 mL of diethyl ether twice. The extracts were dried over magnesium sulfate overnight. The solvent was removed in a rotavapor, and the residue was purified by chromatography on silica gel with the eluent petroleum ether/ethyl ether at 10:0.5. Yield of platinum(II) [4,6-bis(trifluoromethyl)-2-(4-methyl-2-pyridinyl-κN)phenyl-κC],[3-(diphenylphosphino)-1,1,1-trifluoro-2-(trifluoromethyl)-2-propanolato-$\kappa O,\kappa P$] (**15**) was 3.10 g (55.56%) as a yellow solid with no mp until 200 °C. ^{1}H NMR (500 MHz, CD_2Cl_2): δ 2.45 (s, 3H, Me), 2.80 (s, 2H, CH2), 7.10−9.10 (m, 15H, arom-H). ^{19}F NMR (377 MHz, CD_2Cl_2): δ −59.12 (s, 3F, CF_3), − 63.53 (s, 3F, CF_3), − 78.04 (s, 6F, CF_3). ^{31}P NMR (500 MHz, CD_2Cl_2): δ 23.42 (t, $^1J_{PPt}$, 2082.05 Hz). Anal. Calcd for $C_{30}H_{20}F_{12}NOPPt$ (MW: 864.52): C, 41.68; H, 2.33; N, 1.62. Found: C, 41.70; H, 2.48; N, 1.82.

Platinum(II) [4,6-Bis(trifluoromethyl)-2-(4-methyl-2-pyridinyl-κN)phenyl-κC],[3-(di-*tert*-butylphosphino)-1,1,1-trifluoro-2-(trifluoromethyl)-2-propanolato-$\kappa O,\kappa P$] (17). Platinum(II) di-μ-chlorobis[4,6-bis(trifluoromethyl)-2-(4-methyl-2-pyridinyl-κN)phenyl-κC] (**9**) (4.0 g, 0.00374 mol), 4.88 g (0.0150 mol) of 2-[(di-*tert*-butylphosphanyl)methyl]-1,1,1,3,3,3-hexafluoropropan-2-ol (**16**), 7.76 g of a 55−60% solution of tetrabutylammonium hydroxide in water, and 40 mL of THF were refluxed for 2 h under argon atmosphere. The reaction mixture was poured into 200 mL of the water and extracted by 200 mL of diethyl ether twice. The extracts were dried over magnesium sulfate overnight. The solvent was removed in a rotavapor, and the residue was purified by chromatography on silica gel with the eluent petroleum ether/ethyl ether at 10:0.5. Yield of platinum(II) [4,6-bis(trifluoromethyl)-2-(4-methyl-2-pyridinyl-κN)phenyl-κC],[3-(di-*tert*-butylphosphino)-1,1,1-trifluoro-2-(trifluoromethyl)-2-propanolato-$\kappa O,\kappa P$] (**17**) was 1.73 g (28.04%) as a yellow solid with no mp until 200 °C. ^{1}H NMR (500 MHz, CD_2Cl_2): δ 1.10 (s, 18H, Me), 2.30 (s, 3H, Me), 2.50 (s, 2H, CH2), 7.00−8.60 (m, 5H, arom-H). ^{19}F NMR (377 MHz, CD_2Cl_2): δ −54.53 (s, 3F, CF_3), −63.30 (s, 3F, CF_3), −77.55 (s, 6F, CF_3). ^{31}P NMR (500 MHz, CD_2Cl_2): δ 47.29 (t,

(47) Lu, W.; Mi, B.-X.; Chan, M. C. W.; Hui, Z.; Zhu, N.; Lee, S.-T.; Che, C.-M. *Chem. Commun.* **2002**, 206.
(48) Lu, W.; Mi, B.-X.; Chan, M. C. W.; Hui, Z.; Che, C.-M.; Zhu, N.; Lee, S.-T. *J. Am. Chem. Soc.* **2004**, *126*, 4958.

Table 4. Summary of Crystal Data, Data Collection, and Structural Refinement Parameters of 10, 13, 15, and 17

	10	**13**	**15**	**17**
empirical formula	$C_{25}H_{27}F_6NO_2Pt$	$C_{21}H_{13}F_{12}N_3OPt$	$C_{30}H_{20}F_{12}NOPPt$	$C_{26}H_{28}F_{12}NOPPt$
fw	682.57	746.43	864.53	824.55
cryst color, form	gold, rod	gold, irreg. block	gold, irreg. block	lt.yellow, irreg. block
cryst syst	monoclinic	triclinic	triclinic	monoclinic
space group	*C*2/*c*	$P\bar{1}$	$P\bar{1}$	*P*2(1)/*c*
a (Å)	14.633(3)	10.3459(10)	9.6483(8)	8.1234(13)
b (Å)	25.866(6)	10.9225(10)	12.0183(9)	14.108(2)
c (Å)	26.110(6)	11.2004(11)	13.4404(11)	24.683(4)
α (deg)	90	83.1732(18)	91.3790(15)	90.000(3)
β (deg)	93.702(4)	84.3240(17)	107.0130(14	91.664(3)
γ (deg)	90	65.3389(16)	98.4040(15)	90.000(3)
V (Å^3)	9862(4)	1140.38(19)	1470.6(2)	2827.6(8)
Z	16	2	2	4
density (g/cm3)	1.839	2.174	1.952	1.937
abs *μ* (mm^{-1})	5.759	6.271	4.928	5.12
F(000)	5312	708	832	1600
cryst size (mm)	0.25 × 0.06 × 0.06	0.25 × 0.25 × 0.20	0.28 × 0.23 × 0.20	0.14 × 0.20 × 0.20
temp (°C)	−100	−100	−100	−100
scan mode	*ω*	*ω*	*ω*	*ω*
detector	Bruker-CCD	Bruker-CCD	Bruker-CCD	Bruker-CCD
θ_{max} (deg)	28.33	28.3	28.28	28.3
no. obsrvd reflns	31086	6591	9734	45504
no. unique reflns	11534	4999	6653	6908
R_{merge}	0.0386	0.0179	0.0138	0.0362
no. params	645	354	416	391
S[b]	1.046	1.042	1.054	1.086
R indices [$I>2\sigma(I)$][a]	wR2 = 0.088, R1 = 0.041	wR2 = 0.055, R1 = 0.023	wR2 = 0.046, R1 = 0.018	wR2 = 0.053, R1 = 0.024
R indices (all data)[a]	wR2 = 0.098, R1 = 0.070	wR2 = 0.056, R1 = 0.025	wR2 = 0.047, R1 = 0.020	wR2 = 0.058, R1 = 0.034
max diff peak, hole (e/Å^3)	1.805,−1.247	1.414,−1.244	0.562,−1.244	2.060,−0.915

[a] $R1 = \sum||F_o| - |F_c||/\sum|F_o|$, $wR2 = \{\sum[w(F_o^2 - F_c^2)^2]/\sum[w(F_o^2)^2]\}^{1/2}$ (sometimes denoted as R_w^2). [b] $GooF = S = \{\sum[w(F_o^2 - F_c^2)^2]/(n - p)\}^{1/2}$, where *n* is the number of reflections and *p* is the total number of refined parameters.

$^1J_{PPt}$, 1945.8 Hz). Anal. Calcd for $C_{26}H_{28}F_{12}NOPPt$ (MW: 824.54): C, 37.87; H, 3.42; N, 1.70. Found: C, 37.93; H, 3.57; N, 1.89.

OLED Device Fabrication and Characterization. OLED devices were fabricated by the thermal evaporation technique. The base vacuum for all of the thin film deposition was in the range of 10^{-6} Torr. The deposition chamber was capable of depositing eight different films without the need to break the vacuum. Patterned indium tin oxide (ITO) coated glass substrates from Thin Film Devices, Inc. were used. These ITOs are based on Corning 1737 glass coated with 1400 Å ITO coating, with sheet resistance of 30 ohms/square and 80% light transmission. The patterned ITO substrates were then cleaned ultrasonically in aqueous detergent solution. The substrates were then rinsed with distilled water followed by 2-propanol and then degreased in toluene vapor.

The cleaned, patterned ITO substrate was then loaded into the vacuum chamber, and the chamber was pumped down to 10^{-6} Torr. The substrate was then further cleaned using an oxygen plasma for about 5 min. After cleaning, multiple layers of thin films were then deposited sequentially onto the substrate by thermal evaporation. Patterned metal electrodes (Al or LiF/Al) or bipolar electrodes were deposited through a mask. The thickness of the film was measured during deposition using a quartz crystal monitor. The completed OLED device was then taken out of the vacuum chamber and characterized immediately without encapsulation.

The OLED samples were characterized by measuring their (1) current−voltage (I−V) curves, (2) electroluminescence radiance versus voltage, and (3) electroluminescence spectra versus voltage. The I−V curves were measured with a Keithley Source measurement unit model 237. The electroluminescence radiance (in the unit of cd/m^2) versus voltage was measured with a Minolta LS-110 luminescence meter, while the voltage was scanned using the Keithley SMU. The electroluminescence spectrum was obtained by collecting light using an optical fiber, through an electronic shutter, dispersed through a spectrograph, and then measured with a diode array detector. All three measurements were performed at the same time and controlled by a computer. The efficiency of the device at certain voltage is determined by dividing the electroluminescence radiance of the LED by the current density needed to run the device. The unit is in cd/A.

Acknowledgment. The authors wish to thank Kurt Adams for funding X-ray research.

Supporting Information Available: The crystallographic information files (CIF) of compounds **10**, **13**, **15**, and **17** are available free of charge via the Internet at http://pubs.acs.org.

OM049211T